Australasian Physical & Engineering Sciences in Medicine (2019) 42:489–502
https://doi.org/10.1007/s13246-019-00745-6

SCIENTIFIC PAPER

Effect of computed tomography number-relative electron density conversion curve on the calculation of radiotherapy dose and evaluation of Monaco radiotherapy treatment planning system

Mohsen Hasani[1] · Bagher Farhood[2] · Mahdi Ghorbani[3] · Hamideh Naderi[4] · Sepideh Saadatmand[4] · Saeed Karimkhani Zandi[4] · Courtney Knaup[5]

Received: 26 May 2018 / Accepted: 27 February 2019 / Published online: 8 March 2019

Abstract

The accuracy of a computed tomography (CT)-relative electron density (RED) curve may have an indirect impact on the accuracy of dose calculation by a treatment planning system (TPS). This effect has not been previously quantified for input of different CT-RED curves from different CT-scan units in the Monaco TPS. This study aims to evaluate the effect of CT-RED curve on the dose calculation by the Monaco radiotherapy TPS. Four CT images of the CIRS phantom were obtained by different CT scanners. The accuracy of the dose calculation in the three algorithms of the Monaco TPS (Monte Carlo, collapse cone, and pencil beam) is also evaluated based on TECDOC 1583. The CT-RED curves from the CT scanners were transferred to the Monaco TPS to audit the different algorithms of the TPS. The dose values were measured with an ionization chamber in the CIRS phantom. Then, the dose values were calculated by the Monaco algorithms in the corresponding points. For the Monaco TPS and based on TECDOC 1583, the accuracy of the dose calculation in all the three algorithms is within the agreement criteria for most of the points evaluated. For low dose regions, the differences between the calculated and measured dose values are higher than the agreement criteria in a number of points. For the majority of the points, the algorithms underestimate the calculated dose values. It was also found that the use of different CT-RED curves can lead to minor discrepancies in the dose calculation by the Monaco TPS, especially in low dose regions. However, it appears that these differences are not clinically significant in most of the cases.

Keywords CT-RED curve · Radiotherapy · Treatment planning system · Audit · Monaco

Introduction

The process of radiotherapy is complex and includes a series of steps. The treatment procedure begins with patient diagnosis and disease staging and culminates in treatment of a determined target volume with proper beam parameters, radiation energies and treatment techniques. The accuracy in each of these steps has a direct effect on the treatment outcome. In order to obtain such accuracy, the discrepancies in all the steps of the radiotherapy process must be reduced as far as possible [1, 2].

Treatment planning system (TPS) is a main component in the radiotherapy process, as its accuracy is essential for a treatment success [3]. A factor that can affect the dose accuracy calculated by a TPS is the accurate calibration of the computed tomography (CT) number to the relative electron density (RED) curve [4]. RED is the electron density of a specific medium related to the electron density of

✉ Bagher Farhood
bffarhood@gmail.com

✉ Mahdi Ghorbani
mhdghorbani@gmail.com

1 Department of Radiotherapy Physics, Cancer Research Centre, Cancer Institute, Tehran University of Medical Sciences, Tehran, Iran

2 Department of Medical Physics and Radiology, Faculty of Paramedical Sciences, Kashan University of Medical Sciences, Kashan, Iran

3 Cancer Research Center, Shahid Beheshti University of Medical Sciences, Tehran, Iran

4 Department of Radiotherapy Physics, Cancer Institute, Qom University of Medical Sciences, Qom, Iran

5 Comprehensive Cancer Centers of Nevada, Las Vegas, NV, USA

water. This quantity is an important factor in dose calculation by TPSs and is generally acquired from CT information [5]. To describe this effect more precisely, it can be noted that pair production interaction is dominant in the range of therapeutic energy, and the electron density obtained from CT-RED curve can be used for determining compositions of materials and the dose is calculated by knowing compositions of materials [6]. Therefore, input of different CT-RED curves from different CT scanners may result in different estimation of material compositions and therefore in different dose distributions in a TPS. On the other hand, CT numbers may vary between various CT scanners [7–12]. In some radiotherapy centers, CT images of patients for the treatment planning process can be provided by different diagnostic centers whose CT-RED is not calibrated for the TPS. Subsequently, this issue can affect the dose calculation by the TPS, which to the best of our knowledge, has not been previously investigated.

A number of guidelines and protocols have been developed in the past years for the systematic quality assurance (QA) of three dimensional TPSs, presenting recommendations for particular QA aspects of a TPS like dose calculation, beam description, anatomical characterization, and data output and transfer [5, 13–16]. The International Atomic Energy Agency (IAEA) has provided a general framework and large number of practical clinical tests for TPSs, in the form of Technical Reports Series (TRSs) No. 430, to help users to verify the dosimetric accuracy of their TPSs [14]. Large radiotherapy centers with limited personnel and high patient load or small radiotherapy centers with limited resources are not always capable of carrying out all tests recommended in this report. The IAEA has published another set of practical clinical tests for TPS users which is a dedicated technical report called TECDOC 1583 [5]. Additionally, there are several TPS commissioning recommendations which have discussed CT calibration curve [14, 17, 18] and recommended tolerances for Hounsfield unit or RED values used in a CT-RED calibration curve [15, 19–21]. In one of the reports by the IAEA, it was mentioned that a variation of ± 60 Hounsfield units can lead to $\pm 1\%$ discrepancy in calculated dose for a 6 MV energy photon beam passing 5 cm of a bone equivalent material [5]. Furthermore, a recent systematic review reported Hounsfield unit tolerances of 20 Hounsfield units for soft tissue and ± 50 Hounsfield units for air and bone corresponding to 1% or lower change in a TPS-calculated dose [22].

Inness et al. [23] calibrated CT-RED data using phantoms and evaluated the effect of phantom geometry on electron density conversion and dose in a TPS. Their results showed that the CT number depended on the type and amount of scattering materials. Their conclusion was that a phantom used for calibration of CT-RED curve should have sufficient water equivalent materials surrounding the heterogeneities in the phantom. Cozzi et al. [24] evaluated the effect of a calibration table which was provided by a manufacturer on dose calculation when the in-center calibration was performed for a TPS. The impact of CT imaging parameters was also evaluated. The maximum error in the monitor units per Gy was about 2%. The applied voltage had the most impact and led to errors in the Hounsfield numbers for high density materials. Although these two studies evaluated the effect of CT-RED calibration on planned dose, they did not evaluate this effect for different CT-scan units. This effect is the subject of evaluation in this study.

The Monaco TPS is used in some radiotherapy centers. This system provides high-quality radiotherapy treatment plans for different radiotherapy modalities. It provides fast calculation speed, accurate Monte Carlo algorithm, and reduced planning time [25].

Several studies have been carried out previously to investigate the dosimetric verification of the Monaco TPS [26–30]. However, in these studies, the dosimetric accuracy of the TPS has been evaluated for specific treatment plans (for example, prostate, head and neck, lung, etc.) or some practical clinical tests presented by TECDOC 1583. In this study the TPS is evaluated based on TECDOC 1583. Kragl et al. [26] compared the dosimetric accuracy of the X-ray voxel Monte Carlo code in the Monaco TPS for flattened and unflattened photon beams. In their study, they evaluated some practical clinical tests presented by TECDOC 1583 and intensity modulated radiation therapy (IMRT) plans for head and neck, prostate, and cervix. Additionally, their results showed that the dose calculation accuracy of the TPS in both the flattened and unflattened modes was within the agreement criteria for the evaluated test cases and IMRT plans. In another study, López-Tarjuelo et al. [28] investigated the dose calculation accuracy of the Monaco TPS for a test set in water, inhomogeneous phantoms, and IMRT verifications. Their findings revealed that dose calculation in a water phantom was in accordance with the measurements, as in 95% of the cases, the differences were up to 1.9%. Moreover, dose calculation in the inhomogeneous phantom demonstrated acceptable results. Li et al. [29] evaluated the dose calculation accuracy of the Monaco TPS (with finite size pencil beam and X-ray voxel Monte Carlo algorithms) in a lung-chest phantom for esophagus cancer planned by IMRT technique. They concluded that the Monte Carlo-based algorithm had more accurate dose calculation in IMRT plans with heterogeneity correction for esophagus cancer. Saenz et al. [30] assessed the dose calculation accuracy of the Monaco TPS (with Monte Carlo algorithm) for radiosurgery plans in the brain. 3D global gamma analysis (3%/2 mm) for film measurement showed passing rates more than 95.0%. Furthermore, 3D global gamma analysis (3%/2 mm) by gel dosimetry demonstrated passing rates of more than 90.0% for most targets.

The current study aims to evaluate the dosimetric accuracy of different algorithms of the Monaco TPS based on all the practical clinical tests presented by TECDOC 1583 (except for the case No. 5). To this end, the evaluation of dosimetric accuracy is performed in the presence of different organs such as lung, bone, and soft tissue. In addition, the effect of CT-RED curves obtained from different CT-scan units is investigated on the dose calculated by the Monaco TPS.

Materials and methods

CIRS phantom

As previously mentioned, the dosimetric accuracy of the Monaco TPS was carried out based on TECDOC 1583 by IAEA [5]. In this document, the recommended phantom is the CRIS phantom (CIRS Inc., Norfolk, Virginia). The phantom has an elliptical shape with dimensions of 30 cm (long) × 30 cm (wide) and thickness of 20 cm. It represents an average human trunk in density and proportion. This phantom is made of plastic bone, lung, and water sections containing 10 holes to insert an ionization chamber. The CIRS phantom was also used to investigate the effect of CT-RED curves on the dose calculated by the Monaco TPS. Dose measurements were carried out by insertion of the calibrated ionization chamber inside various holes of the CIRS phantom.

Practical clinical tests

All practical clinical tests presented by TECDOC 1583 (except for the case No. 5) were applied for the evaluations. These tests consist of eight clinical test cases which are described in details in the TECDOC 1583 [5]. Figure 1 illustrates the positions of measurement points in the CIRS phantom as well as sample dose distributions and beam geometries for all the practical clinical tests. The reason for not performing the test case No. 5 is that there were not enough facilities to perform this test case. The aim of the test No. 1 is to verify the dose calculation of a TPS for the reference field (i.e., 10×10 cm^2). The test No. 2 verifies the dose calculation of the TPS in the case of lack of scattering for a tangential field. The purpose of the test No. 3 is to verify the dose calculation of the TPS for a blocked field. The test No. 4 simulates radiotherapeutic treatments such as prostate and its aim is to verify the dose calculation delivered with an individual beam and total dose from four fields which are weighted equally. The aim of the test No. 6 is to verify the

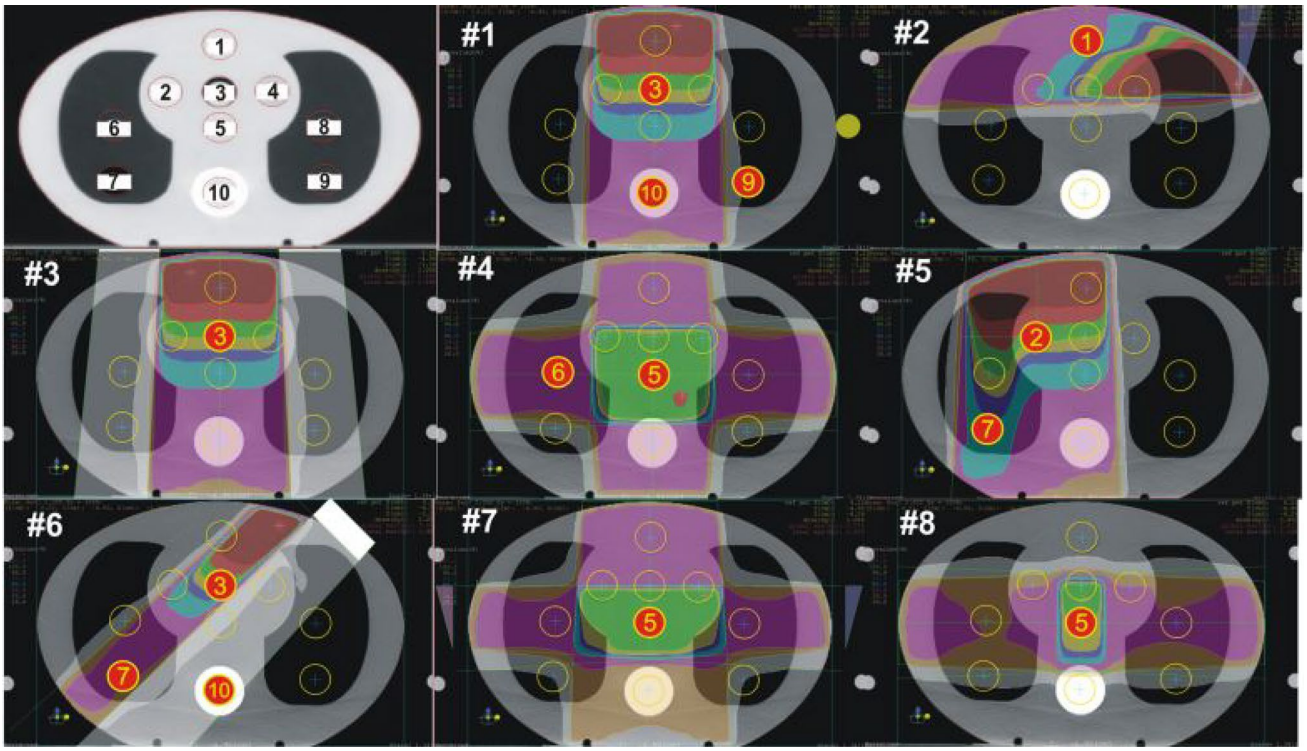

Fig. 1 Positions of the measurement points in the CIRS phantom for practical clinical tests presented by TECDOC 1583. Beam geometry and sample dose distribution for all the test cases are also shown. Permission from Rutonjski [35]. It is noteworthy that the parts No. 1 to No. 8 represent the test cases No 1–8, respectively

dose calculation of TPS for irregular fields with blocking of the center of the fields. The effect of oblique beam incidence on dose calculation accuracy is also evaluated with this test. The test No. 7 verifies the TPS dose calculation for wedged paired fields and asymmetric collimation. The purpose of the test No. 8 is to verify the dose calculation of the TPS with rotation of collimator and couch.

It is notable that measurement points for each test case are chosen to avoid measurements in the penumbra and high dose gradient regions. The total number of measurement points in the CIRS phantom was 13 for the seven test cases.

Different CT scanners, the Monaco TPS algorithms and dose calculation

Four CT image series of the CIRS phantom were obtained by four various CT scanners in four cities of Iran. The CT scanners used in the cities of Tehran, Qom, Hamadan, and Birjand are GE Lightspeed Pro 16 slice (GE Medical Systems, Milwaukee, WI, USA), Neusoft 16 slice (Neusoft Medical System Co., Ltd., Shenyang, China), Toshiba Aquilion 16 slice (Toshiba Medical Systems, Tokyo, Japan), and Siemens Somatom 16 slice (Siemens Medical Solutions, Forchheim, Germany), respectively. The other properties of the CT scanners are presented in Table 1. These scanners were routinely calibrated based on the report by the task group No. 12 [31] in their imaging departments. Given that the information related to the CT numbers and RED values of the materials used in the CT calibration phantoms have been provided by the companies, hence, the CT-RED curves were evaluated using the tolerance provided by the relevant standard guidelines [5, 14, 19, 21]. The obtained results were within the agreement criteria and the CT-RED curves were accepted to be entered in the TPS dose calculation. However, if the differences obtained for the CT-RED curve were greater than tolerance values, the CT scanners were re-calibrated. The CT-RED curves obtained from these four CT scanners are plotted in Fig. 2. Moreover, CT numbers and RED values for the GE Lightspeed Pro (Tehran), Neusoft (Qom), Toshiba Aquilion (Hamadan), and Siemens Somatom (Birjand) CT scanners are listed in Table 2. These images were transported to the Monaco TPS at the Sadra Radiotherapy Center (Qom, Iran) and then treatment

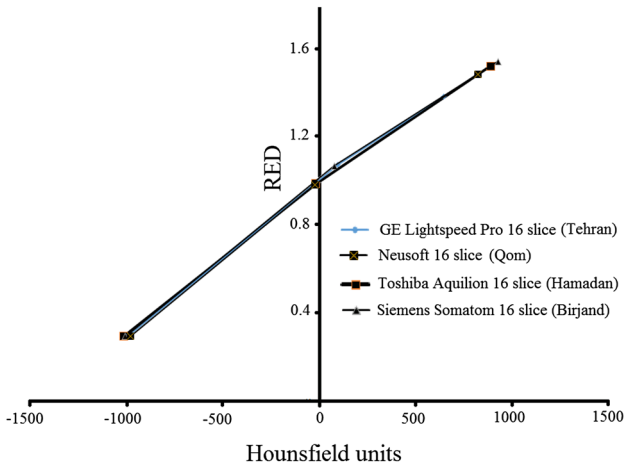

Fig. 2 CT-RED curves obtained from the GE Lightspeed Pro (Tehran), Neusoft (Qom), Toshiba Aquilion (Hamadan), and Siemens Somatom (Birjand) CT scanners

planning was performed for each of the test cases based on the TECDOC 1583. Finally, for each of the test cases and all the four CT image series, dose calculation were carried out by various algorithms of the TPS in specific holes, which are described in details in Table 3 [5]. For dose calculation, circular regions of interest (ROI) with the diameter of 10 mm were specified on these CT images within the specific holes, and mean dose values for these holes were obtained by the Monaco TPS. It is noteworthy that the ROIs selected for the dose value measurements were less than the physical area of the holes, and they had sufficient distance to the boundaries of the holes.

In the current study, three different calculation algorithms of the Monaco TPS (version 5.10.02, Elekta AB, Stockholm, Sweden) were investigated. These algorithms are Monte Carlo, collapse cone, and pencil beam. Monaco has various algorithms for dose calculation: X-ray voxelized Monte Carlo for treatment by photons for different modalities, graphical processing unit Monte Carlo for treatment by photons for different modalities, collapsed cone convolution treatment by photons, voxelized Monte Carlo++ for treatment by electrons, and carbon pencil beam spot for treatment by carbon spot. A more detailed description of such algorithms is mentioned in

Table 1 The CT scanners properties used in this study

CT scanner type	Tube voltage (kVp)	Current (mAs)	Field of view (cm)
GE Lightspeed Pro 16 slice (Tehran)	110	110	50
Neusoft 16 slice (Qom)	120	100	40
Toshiba Aquilion 16 slice (Hamadan)	120	100	50
Siemens Somatom 16 slice (Birjand)	110	120	38

The reconstruction algorithm used in all the scanners is backprojection

Table 2 The CT numbers and RED for the GE Lightspeed Pro (Tehran), Neusoft (Qom), Toshiba Aquilion (Hamadan), and Siemens Somatom (Birjand) CT scanners

Tissue type	Hamadan		Tehran		Birjand		Qom	
	CT number	RED	CT number	RED	CT number	RED	CT number	RED
Air	− 1013	0.22	− 993	0.22	− 1004	0.22	− 978	0.22
Soft tissue	− 16	0.98	98	1.07	80	1.06	− 21	0.98
Bone	891	1.52	978	1.62	930	1.58	825	1.49

Table 3 Geometries for different test cases used in the current study (extracted from TECDOC 1583 [5])

Test case no.	Number of beams	Set-up type	Reference point	Measurement point	Field size (cm^2)	Gantry angle	Collimator angle	Beam modifiers
1	1	SSD = SAD	3	3 9 10	10 × 10	0	0	None
2	1	SAD	1	1	15 × 10	90	0	45 degree wedge
3	1	SSD = SAD	3	3	14 × 14 shaped to 10 × 10	0	45	Blocks
4	4	SAD	5	5 6 10	15 × 10 Ant 15 × 10 Post 15 × 8 RL 15 × 8 LL	0 180 270 90	0 0 0 0	None
6	1	SAD	3	3 7 10	L-shaped 10 × 20	45	90	Custom block
7	3	SAD	5	5	10 × 12 10 × 6 asymmetric 10 × 6 asymmetric	0 90 270	0	None Physical wedge 30° Physical wedge 30°
8	3	SAD	5	5	4 × 16 LL 4 × 16 RL 4 × 4 (table 270)	90 270 30	330 30 0	None

the literature [25]. The size of the grid implemented in all the algorithms of dose calculation is 2 mm.

Dose measurements

Dose measurements were carried out at the Sadra Radiotherapy Center by irradiation of an Elekta Synergy Platform linear accelerator (Elekta Ltd, Stockholm, Sweden) with nominal photon energies of 6 and 18 MV. A calibrated ionization chamber (TM30013-0021 type; PTW, Freiburg, Germany) was used for the dose measurements. This chamber was calibrated for dosimetric purposes by a secondary standards dosimetry laboratory (SSDL) which is traceable to the Iranian Atomic Energy Agency. Finally, the dose measurements were carried out three times for each of the test cases by insertion of the calibrated ionization chamber inside the specific holes of the phantom. It is noteworthy that for all the dose measurement points, the absorbed dose to water was obtained from ionization chamber measurements by using the TRS No. 398 dosimetry protocol [32].

Data analysis

The calculated (D_{Calc}) and measured (D_{Meas}) doses were obtained for the same points in each of the seven clinical test cases. The percent differences between D_{Calc} and D_{Meas} values (δ (%)) were specified for these points. To have better consistency in description of the findings for different points, the dose differences were normalized to the measured dose at the reference point ($D_{Meas, Ref}$) for each of the test cases. The reference point was a point that received 200 cGy dose and it was determined for each test case.

Based on the evaluation of the repeated results of in-phantom measurements, the uncertainty over all the dose measurements was less than 1%. The TPS calculations were also repeated two times and the results for the two calculations were the same. The uncertainties of the dose calculation and measurements have two major components: type A or statistical uncertainty and type B or systematic uncertainty. In the present calculations or measurements, there are various components for the type B uncertainty such as the grid size implemented in the dose calculation algorithms, volume-averaging artifact of dosimeter, measurement of

temperature and pressure, approximations in treatment planning calculations, and some other factors.

Results

The dosimetric accuracy of different Monaco TPS algorithms

Differences between D_{Calc} and D_{Meas} for the different test cases and measurement points for all the four CT image series of the CIRS phantom obtained by GE Lightspeed Pro 16 slice, Neusoft 16 slice, Toshiba Aquilion 16 slice, and Siemens Somatom 16 slice CT scanners are presented in Tables 4, 5, 6 and 7, respectively. The agreement for each of the points studied is listed in the third column of the above-mentioned tables. The agreement criteria in these tables are based on the values reported by the TECDOC No 1583 by IAEA [5].

Effect of CT-RED curves on the dose calculated by the Monaco TPS

The average absolute dose difference between the calculated and measured dose values related to the four CT-RED curves and in-phantom measurements is listed in Table 8. Moreover, in Table 9, dose values calculated by the different algorithms of the Monaco TPS are compared between the four CT image series of the CIRS phantom.

Discussion

In radiotherapy treatment planning, CT images are used for two key purposes: to allow the accurate contouring of the target volume and organs at risk, and to present an accurate map of the electron density of different tissues for dose calculation by the TPS [22]. The Hounsfield units of CT images for various tissue types must not change significantly from the values applied in the CT-RED calibration curve within the TPS. The reason is that by using the TPS calibration, Hounsfield unit values are converted to RED. Therefore, if there is a mismatch between the TPS calibration curve and Hounsfield unit values in the CT image for particular tissue types, it will lead to discrepancies in the dosimetric calculations performed by the TPS [24, 33]. In some radiotherapy centers, it is possible that several CT-RED calibration curves are used within the TPS; in this condition, there is opportunity to apply various CT scanners and CT-scan protocols for various body regions. However, there are limitations in the number of CT-RED calibration curves in some radiotherapy centers, and also in attempt to decrease the risk of incorrect selection of these curves and the work associated with their quality assurance testing [34]. In the current study, the effect of CT-RED curves obtained from different CT-scan units was investigated on the dose calculated by the Monaco TPS. Furthermore, the dosimetric accuracy of different algorithms of the Monaco TPS was evaluated based on practical clinical tests presented by TECDOC 1583 [5].

Table 4 The difference between the measured (D_{Meas}) and calculated (D_{Calc}) doses for different algorithms of the Monaco TPS. The CT images were obtained by GE Lightspeed Pro 16 slice (Tehran, Iran)

Test case	Measurement hole	Agreement criteria (%) [5]	6 MV			18 MV		
			Percentage difference between D_{Meas} and D_{Calc} (δ)			Percentage difference between D_{Meas} and D_{Calc} (δ)		
			Monte Carlo	Collapse cone	Pencil beam	Monte Carlo	Collapse cone	Pencil beam
Case 1	3	2	−0.3	−0.3	−0.3	0.0	0.0	0.0
	9	4	−1.6	−1.1	−3.4	−2.8	−2.2	**−4.6**
	10	3	0.0	−1.0	−1.9	2.3	0.4	−0.9
Case 2	1	3	–	−0.6	–	–	0.3	–
Case 3	3	3	−1.3	−1.3	−1.3	−1.7	−1.7	−1.7
Case 4	5	3	−1.1	−1.1	−1.1	−2.8	−2.8	−2.8
	6	4	−2.1	−4.0	−2.4	−3.2	−3.9	−3.2
	10	4	1.4	1.4	2.5	−2.2	−1.5	−1.2
Case 6	3	3	−0.1	−0.1	−0.1	−1.1	−1.1	−1.1
	7	4	−1.3	−2.4	2.3	−1.9	0.0	**7.8**
	10	5	−0.1	0.4	−3.8	−0.1	−0.2	−1.9
Case 7	5	4	–	−1.3	–	–	−2.0	–
Case 8	5	3	0.2	0.2	0.2	−2.3	−2.3	−2.3

Table 5 The difference between the measured (D_{Meas}) and calculated (D_{Calc}) doses for different algorithms of the Monaco TPS. The CT images were obtained by Neusoft 16 slice (Qom, Iran)

Test case	Measurement hole	Agreement criteria (%) [5]	6 MV			18 MV		
			Percentage difference between D_{Meas} and D_{Calc} (δ)			Percentage difference between D_{Meas} and D_{Calc} (δ)		
			Monte Carlo	Collapse cone	Pencil beam	Monte Carlo	Collapse cone	Pencil beam
Case 1	3	2	−0.3	−0.3	−0.3	0.0	0.0	0.0
	9	4	−2.8	−1.7	**−5.4**	−2.5	−2.4	**−6.9**
	10	3	**−4.5**	−3.0	−1.4	2.0	−0.5	−0.2
Case 2	1	3	–	−0.6	–	–	0.3	–
Case 3	3	3	−1.3	−1.3	−1.3	−1.7	−1.7	−1.7
Case 4	5	3	−1.1	−1.1	−1.1	−2.8	−2.8	−2.8
	6	4	−1.8	−1.7	−2.0	−1.4	−2.1	−2.4
	10	4	0.8	1.0	2.2	−0.9	−1.8	−1.2
Case 6	3	3	−0.1	−0.1	−0.1	−1.1	−1.1	−1.1
	7	4	−2.4	−2.0	1.7	0.1	1.5	**6.5**
	10	5	−0.4	−0.6	−3.7	−0.8	−0.2	−1.9
Case 7	5	4	–	−1.3	–	–	−2.0	–
Case 8	5	3	0.2	0.2	0.2	−2.3	−2.3	−2.3

Table 6 The difference between the measured (D_{Meas}) and calculated (D_{Calc}) doses for different algorithms of the Monaco TPS. The CT images were obtained by Toshiba Aquilion 16 slice (Hamadan, Iran)

Test case	Measurement hole	Agreement criteria (%)	6 MV			18 MV		
			Percentage difference between D_{Meas} and D_{Calc} (δ)			Percentage difference between D_{Meas} and D_{Calc} (δ)		
			Monte Carlo	Collapse cone	Pencil beam	Monte Carlo	Collapse cone	Pencil beam
Case 1	3	2	−0.3	−0.3	−0.3	0.0	0.0	0.0
	9	4	−0.9	0.0	−4.0	−0.9	**−5.0**	**−5.1**
	10	3	**−5.1**	**−3.1**	−1.5	−2.0	−2.0	−0.2
Case 2	1	3	–	−0.6	–	–	0.3	–
Case 3	3	3	−1.3	−1.3	−1.3	−1.7	−1.7	−1.7
Case 4	5	3	−1.1	−1.1	−1.1	−2.8	−2.8	−2.8
	6	4	−0.1	−2.2	−2.0	−0.5	−3.0	−3.0
	10	4	2.2	0.9	2.3	−0.6	−1.8	−1.2
Case 6	3	3	−0.1	−0.1	−0.1	−1.1	−1.1	−1.1
	7	4	1.2	−1.0	2.7	4.0	2.6	**8.6**
	10	5	−0.6	−0.6	−3.6	−0.1	−0.3	−1.8
Case 7	5	4	–	−1.3	–	–	−2.0	–
Case 8	5	3	0.2	0.2	0.2	−2.3	−2.3	−2.3

The dosimetric accuracy of different Monaco TPS algorithms

Generally, from the data in Tables 4, 5, 6 and 7, it is evident that the differences between the Monaco TPS-calculated and in-phantom measured dose values are less than the agreement criteria in most of the test cases. The agreement criteria in these tables are based on the values reported by the TECDOC No 1583 by IAEA [5]. These criteria vary based on the complexity of test cases, and range from 2 to 5%. Data corresponding to differences higher than the agreement criteria are bolded in these tables. These data points are corresponding to the test No. 1, points No. 9 and 10, test No. 6, and point No. 7. Detailed information on the in-phantom locations of these data points and other aspects is discussed in the following.

For the test No. 1, differences between D_{Calc} and D_{Meas} for all the algorithms of the Monaco TPS were almost

Table 7 The difference between the measured (D_{Meas}) and calculated (D_{Calc}) doses for different algorithms of the Monaco TPS. The CT images were obtained by Siemens Somatom 16 slice (Birjand, Iran)

Test case	Measurement hole	Agreement criteria (%)	6 MV			18 MV		
			Percentage difference between D_{Meas} and D_{Calc} (δ)			Percentage difference between D_{Meas} and D_{Calc} (δ)		
			Monte Carlo	Collapse cone	Pencil beam	Monte Carlo	Collapse cone	Pencil beam
Case 1	3	2	−0.3	−0.3	−0.3	0.0	0.0	0.0
	9	4	−2.6	−2.4	−2.4	−3.5	−3.6	−3.2
	10	3	−2.5	**−4.0**	−2.4	−0.8	−2.0	−1.5
Case 2	1	3	–	−0.6	–	–	0.3	–
Case 3	3	3	−1.3	−1.3	−1.3	−1.7	−1.7	−1.7
Case 4	5	3	−1.1	−1.1	−1.1	−2.8	−2.8	−2.8
	6	4	−1.8	−1.8	−2.1	−0.4	−2.7	−2.9
	10	4	0.6	1.3	2.3	−2.7	−1.8	−1.3
Case 6	3	3	−0.1	−0.1	−0.1	−1.1	−1.1	−1.1
	7	4	1.2	−1.2	2.2	2.6	1.9	**8.0**
	10	5	−0.5	−0.2	−3.5	0.6	−0.1	−1.8
Case 7	5	4	–	−1.3	–	–	−1.9	–
Case 8	5	3	0.2	0.2	0.2	−2.3	−2.3	−2.3

Table 8 The average of absolute dose differences (%) between the calculated and measured dose values related to the four CT-RED curves and in-phantom measurements

Model of CT-scan unit	Type of algorithm					
	Monte Carlo	Collapse cone	Pencil beam	Monte Carlo	Collapse cone	Pencil beam
	6 MV			18 MV		
GE Lightspeed Pro 16 slice (Tehran, Iran)	0.79	1.09	1.48	1.63	1.31	2.29
Neusoft 16 slice (Qom, Iran)	1.21	1.06	1.49	1.30	1.34	2.16
Toshiba Aquilion 16 slice (Hamadan, Iran)	1.05	0.91	1.59	1.28	1.78	2.32
Siemens Somatom 16 slice (Birjand, Iran)	0.94	1.13	1.38	1.42	1.59	2.05

within the agreement criteria, except for several points which are bolded in Tables 4, 5, 6 and 7. All the differences range from 0 to 6.9%, as the largest deviation is related to the pencil beam algorithm in 18 MV beam energy. Because of the simplicity of this test (i.e., verifying the TPS-calculated dose for the reference field), the agreement criterion is 2% for the points inside the field (the point 3) and it is accurately calculated by all the three algorithms of Monte Carlo, collapse cone, and pencil beam. Moreover, for low dose regions (the point 9), differences between D_{Calc} and D_{Meas} is higher than the agreement criteria (4%) in the bolded points. Our results are in line with the findings of Rutonjski et al. [35], as they reported that the accuracy of the dose calculation in two different algorithms of CMS XiO (Elekta CMS Software, St. Louis, Missouri) TPSs was within the agreement criteria, but it was not sufficient for low dose regions. In that study, an audit was conducted in three radiotherapy departments of Serbia by CT scanning and measurements in an anthropomorphic phantom and treatment planning was performed for eight test cases based on the IAEA report. However, Kragl et al. [26] stated that the Monte Carlo and enhanced collapsed cone (eCC) algorithms of the Monaco TPS passed the agreement criteria within and outside the radiation field. In that study, the eCC algorithm in Oncentra Masterplan and XVMC (MC) code in the Monaco TPSs was evaluated. Treatment planning was performed for 10 MV photon energy in the cases of flattening filter and flattening filter free beams. Radiochromic films were irradiated in a solid water phantom and evaluated gamma index analysis. A thorax phantom was also used and conformal plans were verified by measurement with ion chambers. IMRT plans were also verified by measurement inside a Delta4 phantom. There are differences between the methods in the study by Kragl et al. [26] and the methods in the present study. For instance, they evaluated the eCC algorithm, a 10 MV photon beam, a flattening free case, and IMRT plans in a Delta4 phantom.

Table 9 Dose values (cGy) calculated by the different algorithms of the Monaco TPS (Monte Carlo, collapse cone, and pencil beam) according to different CT image series of the CIRS phantom obtained by the four various CT scanners of GE Lightspeed Pro 16 slice (1), Neusoft 16 slice (2), Toshiba Aquilion 16 slice (3), and Siemens Somatom 16 slice (4)

Test case	Measurement hole	6 MV											
		Monte Carlo algorithm				Collapse cone algorithm				Pencil beam algorithm			
		1	2	3	4	1	2	3	4	1	2	3	4
Case 1	3	200.0	200.0	200.0	200.0	200.0	200.0	200.0	200.0	200.0	200.0	200.0	200.0
	9	21.9	13.0	16.9	23.9	21.0	15.2	18.5	23.5	11.9	7.9	10.7	13.8
	10	125.5	116.4	115.0	120.4	123.3	119.5	119.1	117.2	121.4	122.7	122.4	120.5
Case 2	1	–	–	–	–	200.0	200.0	200.0	200.0	–	–	–	–
Case 3	3	200.0	200.0	200.0	200.0	200.0	200.0	200.0	200.0	200.0	200.0	200.0	200.0
Case 4	5	200.0	200.0	200.0	200.0	200.0	200.0	200.0	200.0	200.0	200.0	200.0	200.0
	6	26.6	28.6	27.6	28.6	25.6	26.8	26.6	26.8	26.5	26.6	26.6	26.6
	10	27.5	27.1	27.8	27.0	27.4	27.2	27.2	27.5	28.0	27.8	27.9	27.9
Case 6	3	200.0	200.0	200.0	200.0	200.0	200.0	200.0	200.0	200.0	200.0	200.0	200.0
	7	109.6	107.2	114.5	116.5	107.3	108.0	110.1	109.7	116.7	115.4	117.5	116.6
	10	13.1	12.5	12.1	12.2	12.5	12.2	12.1	12.9	6.3	6.0	6.0	5.7
Case 7	5	–	–	–	–	200.0	200.0	200.0	200.0	–	–	–	–
Case 8	5	200.0	200.0	200.0	200.0	200.0	200.0	200.0	200.0	200.0	200.0	200.0	200.0
Test case	Measurement hole	18 MV											
		Monte Carlo algorithm				Collapse cone algorithm				Pencil beam algorithm			
		1	2	3	4	1	2	3	4	1	2	3	4
Case 1	3	200.0	200.0	200.0	200.0	200.0	200.0	200.0	200.0	200.0	200.0	200.0	200.0
	9	28.3	17.6	20.8	29.8	27.1	17.5	23.3	29.9	13.4	8.9	12.4	16.2
	10	142.9	142.0	134.4	136.6	139.0	137.2	137.1	134.2	136.4	137.9	137.8	135.2
Case 2	1	–	–	–	–	200.0	200.0	200.0	200.0	–	–	–	–
Case 3	3	200.0	200.0	200.0	200.0	200.0	200.0	200.0	200.0	200.0	200.0	200.0	200.0
Case 4	5	200.0	200.0	200.0	200.0	200.0	200.0	200.0	200.0	200.0	200.0	200.0	200.0
	6	26.2	27.1	28.1	27.6	25.8	26.8	26.3	26.5	26.2	26.6	26.3	26.4
	10	27.0	27.7	28.5	26.8	27.4	27.3	27.2	27.2	27.5	27.5	27.6	27.5
Case 6	3	200.0	200.0	200.0	200.0	200.0	200.0	200.0	200.0	200.0	200.0	200.0	200.0
	7	110.3	114.4	122.1	119.4	114.1	117.1	119.5	117.7	129.9	127.3	131.6	130.2
	10	9.6	8.3	9.5	11.1	9.5	9.2	9.5	9.4	5.9	6.1	6.2	6.2
Case 7	5	–	–	–	–	200.0	200.0	200.0	200.0	–	–	–	–
Case 8	5	200.0	200.0	200.0	200.0	200.0	200.0	200.0	200.0	200.0	200.0	200.0	200.0

It is notable that the reference point received 200 cGy dose, and it was determined for each test case in Table 3

For the test No. 2, according to Tables 4, 5, 6, and 7, differences between D_{Calc} and D_{Meas} for the collapse cone algorithm was within the agreement criteria (3%) and the deviations for 6 MV beam energy was higher than those for 18 MV beam energy (− 0.6% vs. 0.3%). The results show that the collapse cone algorithm underestimates dose values in 6 MV beam energy but overestimates dose values in 18 MV beam energy. These data are consistent with the findings of several studies [36–38]. Farhood et al. [36] reported that the dose calculation accuracy of TiGRT TPS was sufficient for the central axis and off-axis regions for a physical wedged field. Venselaar and Welleweerd [37] investigated the dose calculation accuracy of seven TPSs for 6, 10, and 18 MV photon beams of two modern linear accelerators. The beam data were the input in the commercial radiotherapy TPSs. They reported that for most TPSs, the dose calculation accuracy in wedged fields was within the tolerance limit. Anjum et al. [38] represented that the accuracy of Eclipse TPS with enhanced dynamic wedges for asymmetric and symmetric fields was sufficient in clinical applications. However, the results presented by Rutonjski et al. [35] were inconsistent with our data, as they reported that for a number of points of the test No. 2, the accuracy of the dose calculation in two different algorithms of CMS XiO TPSs was not within the agreement criteria. The difference between the current study

and Rutonjski et al.'s study may be due to the different algorithms/TPSs used in these two studies.

For the test No. 3, the results (Tables 4, 5, 6, 7) show that differences between D_{Calc} and D_{Meas} for all the three algorithms of the Monaco TPS are within the agreement criteria (3%) and they were the same for all the algorithms in each of the beam energies. The deviations in 18 MV beam energy were higher than those in 6 MV beam energy (− 1.3% vs. − 1.7%). All the three algorithms underestimated dose values for the both beam energies. The dose underestimation can be due to the limitations of the Monaco TPS in modeling the dose contributions from contaminated electrons originating from block and the components of linac's head. These data are consistent with the findings of several studies [2, 26, 35], as they reported that the dose calculation accuracy of algorithms/TPSs implemented in their studies was within the agreement criterion for the test No. 3.

For the test No. 4, the agreement criteria ranged from 2 to 4%. The results related to this test (Tables 4, 5, 6, 7) reveal that differences between D_{Calc} and D_{Meas} for all the algorithms of the Monaco TPS are within the agreement criteria. These differences ranged from 0.15 to 4%, and the largest deviation is related to the collapse cone algorithm in 6 MV beam energy (− 4.0%). For most of the cases, the deviations in 18 MV beam energy are higher than that in 6 MV beam energy. The results presented by Kragl et al. [26] confirm these findings. They reported that the dose calculation accuracy of the algorithms applied in the Monaco TPS in the points No. 5 and 6 of the test No. 4 is within the agreement criteria. However, Gershkevitsh et al. [2] and Rutonjski et al. [35] reported that the dose calculation accuracy of algorithms/TPSs evaluated in their studies was not sufficient for some points of the test No. 4.

For the test No. 6, according to Tables 4, 5, 6, and 7, differences between D_{Calc} and D_{Meas} for all the algorithms of the Monaco TPS are within the agreement criteria, except for several points which are bolded in Tables 4, 5, 6, and 7. For this test, the agreement criteria range from 3 to 5%, as they are 3% and 4% for high and low dose regions within radiation fields respectively, and is 5% for the under block region. The differences range from 0 to 8.6%, as the largest deviation is related to the pencil beam algorithm in 18 MV beam energy. It is noteworthy that for the majority of the points, the dose calculation accuracy of the pencil beam algorithm is worse than the other two. The findings of Krag et al. [26] agreed with our results; accordingly, they reported that the dose calculation accuracy of the algorithms applied in the Monaco TPS in the points No. 3 and 7 of the test No. 6 was within the agreement criteria.

Our findings (Tables 4, 5, 6, 7) for the test No. 7 demonstrate that differences between D_{Calc} and D_{Meas} for the collapse cone algorithm are within the agreement criteria (4%), but are higher for 18 MV beam energy compared to 6 MV beam energy (− 2.0%/− 1.9% vs. − 1.3%). The calculated dose values are also underestimated by this algorithm for the both beam energies. These data are in line with the findings of Krag et al. [26] and Rutonjski et al. [35], as they reported that the dose calculation accuracy of algorithms/TPSs used in their studies was within the agreement criteria for the test No. 7. However, Venselaar and Welleweerd [37] reported that the dose calculation accuracy of seven TPSs implemented in their study for asymmetrically wedged case was outside the agreement criteria. There are differences between the current study and the study conducted by Venselaar and Welleweerd [37], including: (1) different geometries for asymmetrically wedged case, (2) different phantoms (water phantom versus CIRS phantom), and (3) different algorithms/TPSs.

For the test No. 8, differences between D_{Calc} and D_{Meas} values for all the algorithms of the Monaco TPS are within the agreement criteria (3%) and they are the same for all the algorithms in the both beam energies. The deviations in 18 MV beam energy are higher than those in 6 MV beam energy (− 2.3% vs. 0.2%). These results are consistent with the findings of Krag et al. [26] and Rutonjski et al. [35]. They stated that the dose calculation accuracy of algorithms/TPSs implemented in their studies was sufficient for this test. However, Gershkevitsh et al. [2] represented that the dose calculation accuracy of pencil beam convolution-based algorithms evaluated in their work was not satisfactory for all photon energies (4–20 MV). That study included 14 different algorithms or inhomogeneity correction methods in different TPSs.

It has been accepted that the dose calculation accuracy of TPSs in out-of-field regions is poor [39, 40] and because of this, the tolerance for these areas is larger (4%) [5, 14]. There are several factors which can affect poor performance of TPSs in out-of-field regions, including the lack of TPS commissioning for out-of-field regions, limitations of TPSs in modeling dose contributions from contaminated electrons resulting from the collimator assembly, flattening filter, and secondary scattering photons from the linac's head [39–41]. The findings presented in Tables 4, 5, 6 and 7 also demonstrate failures of dose calculation in these regions (the point No. 9 of the test No. 1), especially for the pencil beam algorithm. There are several studies which have quantified the dose calculation accuracy of different TPSs in out-of-field regions [3, 36, 39, 41–43], and these studies reported dose underestimation by different algorithms/TPSs. Other results of the current study (Tables 4, 5, 6, 7) show that for some of the test cases, the dose calculation accuracy of the Monaco TPS for inhomogeneities of lung (the point No. 9) and bone (the point No. 10) is outside the agreement criteria, especially for the pencil beam algorithm and these findings are supported by other recent published studies [2, 35]. Generally, it is suggested that the TPS user should be cautious

when dose calculation by the Monaco TPS is performed in out-of-field and inhomogeneities cases.

The above-mentioned (Monte Carlo, collapse cone, and pencil beam) algorithms for dose calculation are model based algorithms. The Monte Carlo algorithm simulates the transport of millions of particles and photons through matter. This algorithm utilizes fundamental laws of physics to obtain probability distributions of individual interactions of particles and photons. This issue was discussed in more details in some reports (TG-105). The Monte Carlo algorithm is the highest accuracy method for treatment planning [44]. The collapse cone algorithm is a convolution-superposition-based method. This method consists of a convolution equation that separately considers the transport of primary photons and that of the scattered electrons and photons emerging from the primary photon interactions. In this algorithm, primarily, a point kernel convolution/superposition model is used and it accounts for density changes in the patient. In this method, variations in lateral photon and electron transport are approximately modeled [2, 35, 44]. In the pencil beam algorithm, the dose distribution in infinitesimally narrow beams is calculated. In this method, the treatment field is divided into a fine grid and the pencil beams are located on the grid along ray lines emerging from the virtual source location defining the beam geometry. The dose distribution in individual pencil beams is calculated, considering all the interactions and medium inhomogeneities. Finally, the dose at any point is obtained by summation of the dose contribution of all the pencils to the point of interest. However, in the pencil beam algorithm, variations in photon transport and lateral electrons are not modeled [2, 35, 44]. By analyzing the results (Tables 4, 5, 6, 7, 8) based on algorithm type implemented on the Monaco TPS, it was observed that the dose calculation accuracy of the pencil beam algorithm is lower than that of the Monte Carlo and collapsed cone ones, especially in the cases of inhomogeneities, which can be due to not adequately considering changes in electron transport in the bone and lung by the pencil beam algorithm. The dose calculation accuracy by the Monte Carlo and collapse cone algorithms is approximately the same and the results obtained by these two algorithms were within the agreement criteria for the majority of the test cases.

The task group (TG) No. 105 of American association of physicist in medicine (AAPM) has published a report on Monte Carlo (MC)-based TPSs for electron and photon beams. In that report, it was mentioned that many research studies announced that MC calculated accurate dose distributions for clinical radiotherapy, particularly in heterogeneous cases where the electron transport effects could not be accurately considered in conventional algorithms of dose calculation. However, long calculation times required by MC algorithms make them impractical for routine clinical treatment planning. Development of faster codes and improvements in computer technology have reduced the calculation times to within minutes on a single processor. These advances became a motivation for treatment planning provides to make attention to MC techniques. Several providers have already introduced or are releasing such algorithms for calculations for photon and electron beams. Therefore, application of MC treatment planning algorithms will be widespread in the radiotherapy community. The TG-105 report provides a review on the studies on MC simulation in radiotherapy planning, and on the issues related to clinical implementation and experimental verification of MC algorithms [45].

Sources of differences between measurements and calculations may arise from a number of factors including: (a) uncertainties involved in the measurements, (b) the TPS beam data input, (c) fitting of the beam model, (d) the dose calculation algorithm, etc. Factors such as inadequacies in input data, dose calculation grid size, choice of phantom type, etc. may affect the dose calculation accuracy of TPSs.

Effect of CT-RED curves on the dose calculated by the Monaco TPS

According to different guidelines [5, 14, 15, 19–21, 46], there are a range of RED values for air, soft tissue and bone, and different tolerances of Hounsfield unit values have been reported for these materials. Given that there is no unique protocol for CT-RED curves, none of the CT-RED curves from different CT scanners is considered as the standard. Furthermore, different CT-scan phantoms were used to obtain CT-RED curves of different CT scanners; hence, we were not able to precisely compare different curves. However, all CT-RED curves were within the agreement criteria. As it can be observed from the results of the average of absolute dose differences between the calculated and measured dose values related to the four CT-RED curves in Table 8, it is evident that the dose calculation accuracy of the Monaco TPS for different CT scanners is approximately the same in most of the cases and the small variation in the obtained data between the scanners is clinically unremarkable. Except for the type of the CT scanner and CT calibration phantom, all the other factors are similar, and the difference between these dose differences can be only attributed to the accuracy of the CT-RED curve. To minimize the related uncertainties in the process of treatment planning for patients, it is recommended that when using patient images from an external CT unit for the purpose of treatment planning, a validation of CT-RED curves of that CT unit be performed before clinical use of the images.

Table 9 presents a more detailed analysis from the results between the four CT image series of the CIRS phantom obtained by the four various CT scanners. For 6 MV

beam energy and within field regions, 0–4.2%, 0–1.3%, and 0–0.9% dose difference ranges were found between the four different CT image series for the Monte Carlo, collapse cone, and pencil beam algorithms, respectively. However, for 18 MV beam energy, 0–5.1%, 0–2.3%, and 0–1.7% dose difference ranges are obtained between the four different CT image series for the Monte Carlo, collapse cone, and pencil beam algorithms, respectively. Moreover, for 6 MV beam energy and outside field regions, 0–29.5%, 0–21.4%, and 0–27.2% dose difference ranges were obtained between the four different CT image series for the Monte Carlo, collapse cone, and pencil beam algorithms, respectively. Yet for 18 MV beam energy, 0.35–25.74%, 0–2.31%, and 0–29.08% dose difference ranges were obtained for the algorithms, respectively. These discrepancies can be attributed to difference in CT-RED curves. To describe this effect more precisely, differences in the properties of the CT scanners such as tube current, tube voltage, size of field of view, and reconstruction algorithms used in the CT scanners may lead to different CT numbers and these numbers can affect the dose calculated by the TPS [7–12]. In this regard, several researchers have studied the dosimetric effect of variation in CT numbers on dose calculation in TPSs [10, 23, 24, 47]. In a study by Inness et al. [23], the dependence of CT-RED conversion on phantom geometry and its effect on dose calculated by Eclipse TPS was evaluated. Cozzi et al. [24] reported that when a CT-RED calibration curve presented by the manufacturer was utilized instead of performing an in-house CT-RED calibration, the largest inaccuracy in monitor units per Gy was 2%. In another study, Nobah et al. [10] investigated the effect of various geometrical arrangements of inserts inside a heterogeneous phantom. They reported that tube voltage and geometrical arrangement caused remarkable differences in Hounsfield unit values.

Conclusion

In the current study, the dose calculation accuracy of three algorithms (Monte Carlo, collapse cone, and pencil beam) used in the Monaco TPS is investigated based on practical clinical tests presented by TECDOC 1583. The accuracy of the dose calculation in the Monte Carlo, collapse cone, and pencil beam algorithms is within the agreement criteria for most of the points evaluated in this study. Furthermore, for the majority of the points, the algorithms underestimate the calculated dose values. Generally, it is suggested that the TPS user should be cautious when performing dose calculation by the Monaco TPS in out-of-field and inhomogeneities cases, especially for the pencil beam algorithm. It is noteworthy that knowing the limitations of the Monaco TPS can help clinicians to make appropriate clinical decisions (for example, in patients with implantable cardiac pacemakers or pregnant patients).

It is also determined that use of different CT-RED curves can lead to minor discrepancies in the dose calculation by the Monaco TPS, especially in low dose regions. However, it appears that these differences are not clinically significant in most of the cases. To minimize the related uncertainties in the process of treatment planning for patients, it is recommended that when using patient images from an external CT unit for the purpose of treatment planning, a validation of CT-RED curve of that CT unit be performed before clinical use of the images.

Acknowledgements The authors would like to thank Shahid Beheshti University of Medical Sciences for financial support of the current study.

Compliance with ethical standards

Conflict of interest There is no conflict of interest.

Ethical approval This study does not involve any evaluation of human or animal samples performed by the authors.

References

1. Van Dyk J, Barnett R, Cygler J, Shragge P (1993) Commissioning and quality assurance of treatment planning computers. Int J Radiat Oncol Biol Phys 26(2):261–273
2. Gershkevitsh E, Schmidt R, Velez G, Miller D, Korf E, Yip F et al (2008) Dosimetric verification of radiotherapy treatment planning systems: Results of IAEA pilot study. Radiother Oncol 89(3):338–346
3. Bahreyni Toossi MT, Farhood B, Soleymanifard S (2017) Evaluation of dose calculations accuracy of a commercial treatment planning system for the head and neck region in radiotherapy. Rep Pract Oncol Radiother 22(5):420–427
4. Constantinou C, Harrington JC, DeWerd LA (1992) An electron density calibration phantom for CT-based treatment planning computers. Med Phys 19(2):325–327
5. International Atomic Energy Agency (2008) Commissioning of radiotherapy treatment planning systems: testing for typical external beam treatment techniques, TECDOC No 1583. International Atomic Energy Agency, Vienna
6. Knöös T, Nilsson M, Ahlgren L (1986) A method for conversion of Hounsfield number to electron density and prediction of macroscopic pair production cross-sections. Radiother Oncol 5(4):337–345
7. Millner MR, McDavid WD, Waggener RG, Dennis MJ, Payne WH, Sank VJ (1979) Extraction of information from CT scans at different energies. Med Phys 6(1):70–71
8. Guan H, Yin FF, Kim JH (2002) Accuracy of inhomogeneity correction in photon radiotherapy from CT scans with different settings. Phys Med Biol 47(17):223–231
9. Ebert MA, Lambert J, Greer PB (2008) CT-ED conversion on a GE Lightspeed-RT scanner: influence of scanner settings. Aust Phys Eng Sci Med 31(2):154–159
10. Nobah A, Moftah B, Tomic N, Devic S (2011) Influence of electron density spatial distribution and X-ray beam quality during CT

simulation on dose calculation accuracy. J Appl Clin Med Phys 12(3):80–89
11. Baxter BS, Sorenson JA (1981) Factors affecting the measurement of size and CT number in computed tomography. Invest Radiol 16(4):337–341
12. Groell R, Rienmueller R, Schaffler GJ, Portugaller HR, Graif E, Willfurth P (2000) CT number variations due to different image acquisition and reconstruction parameters: a thorax phantom study. Comput Med Imaging Graph 24(2):53–58
13. Fraas B, Doppke K, Hunt M (1998) Quality assurance for clinical radiotherapy treatment planning, AAPM Radiation Therapy committee TG53. Med Phys 25(10):1773–1829
14. Andreo P, Cramb J, Fraass B, Ionescu–Farca F, Izewska J, Levin V et al (2004) Commissioning and quality assurance of computerized planning systems for radiation treatment of cancer, Technical Report Series 430. International Atomic Energy Agency, Vienna
15. Mijnheer B, Olszewska A, Fiorino C, Hartmann G, Knöös T, Rosenwald JC et al (2004) Quality assurance of treatment planning systems: practical examples for non-IMRT photon beams. ESTRO, Brussels
16. International Atomic Energy Agency (2007) Specification and acceptance testing of radiotherapy treatment planning systems, TECDOC No 1540. International Atomic Energy Agency, Vienna
17. Venselaar J, Welleweerd H, Mijnheer B (2001) Tolerances for the accuracy of photon beam dose calculations of treatment planning systems. Radiother Oncol 60(2):191–201
18. American Association of Physicists in Medicine Task Group 65 of the Radiation Therapy Committee. Report 85 (2004) Tissue inhomogeneity corrections for megavoltage photon beams. Medical Physics Publishing, Madison
19. Thomson E, Edyvean S (1999) Sect. 3.2. In: IPEM Report 88. Physical aspects of quality control in radiotherapy. York, UK. Institute of Physics and Engineering in Medicine
20. Bissonnette JP, Balter P, Dong L, Lovelock M, Miften M, Moseley D et al (2012) Quality assurance for image guided radiation therapy utilizing CT-based technologies: a report of the AAPM TG-179. Med Phys 39(4):1946–1963
21. IAEA (2012) IAEA Human Health Series No 19, Quality Assurance for Computed Tomography. Diagnostic and Therapy Applications, IAEA, Vienna
22. Davis AT, Palmer AL, Nisbet A (2017) Can CT scan protocols used for radiotherapy treatment planning be adjusted to optimize image quality and patient dose? A systematic review. Br J Radiol 90(1076):20160406
23. . Inness EK, Moutrie V, Charles PH (2014) The dependence of computed tomography number to relative electron density conversion on phantom geometry and its impact on planned dose. Aust Phys Eng Sci Med 37(2):385–391
24. Cozzi L, Fogliata A, Buffa F, Bieri S (1998) Dosimetric impact of computed tomography calibration on a commercial treatment planning system for external radiation therapy. Radiother Oncol 48(3):335–338
25. Clements M, Schupp N, Tattersall M, Brown A, Larson R (2018) Monaco treatment planning system tools and optimization processes. Med Dosim 43(2):106–117
26. Kragl G, Albrich D, Georg D (2011) Radiation therapy with unflattened photon beams: dosimetric accuracy of advanced dose calculation algorithms. Radiother Oncol 100(3):417–423
27. Boggula R, Jahnke L, Wertz H, Lohr F, Wenz F (2011) Patient-specific 3D pretreatment and potential 3D online dose verification of Monte Carlo-calculated IMRT prostate treatment plans. Int J Radiat Oncol Biol Phys 81(4):1168–1175
28. Lopez-Tarjuelo J, Garcia-Molla R, Juan-Senabre X, Quirós-Higueras J, Santos-Serra A, de Marco-Blancas N et al (2014) Acceptance and commissioning of a treatment planning system based on Monte Carlo calculations. Technol Cancer Res Treat 13(2):129–138
29. Li X, Xu B, Lei Y, Zhang J, Lin Z, Li S (2018) Evaluation of dose calculations with inhomogeneity correction in intensity-modulated radiation therapy for esophagus cancer. J X-Ray Sci Technol 26(4):657–666
30. Saenz DL, Li Y, Rasmussen K, Stathakis S, Pappas E, Papanikolaou N (2018) Dosimetric and localization accuracy of Elekta high definition dynamic radiosurgery. Phys Med 54:146–151
31. Shepard SJ, Lin PJP, Boone JM, Cody DD, Fisher JR, Frey GD et al (2002) AAPM Report No. 74: Quality control in diagnostic radiology, Report of task group No. 12 diagnostic X-ray imaging committee. Medical Physics Publishing, Madison
32. Andreo P, Burns DT, Hohlfeld K, Huq MS, Kanai T, Laitano F et al (2000) Absorbed dose determination in external beam radiotherapy: an international code of practice for dosimetry based on standards of absorbed dose to water. IAEA TRS 398, Vienna
33. Craig T, Brochu D, Van Dyk J (1999) A quality assurance phantom for three-dimensional radiation treatment planning. Int J Radiat Oncol Biol Phys 44(4):955–966
34. Davis AT, Palmer AL, Pani S, Nisbet A (2018) Assessment of the variation in CT scanner performance (image quality and Hounsfield units) with scan parameters, for image optimisation in radiotherapy treatment planning. Phys Med 45:59–64
35. Rutonjski L, Petrović B, Baucal M, Teodorović M, Čudić O, Gershkevitsh E et al (2012) Dosimetric verification of radiotherapy treatment planning systems in Serbia: national audit. Radiat Oncol 7(1):155–162
36. Farhood B, Bahreyni Toossi MT, Soleymanifard S (2016) Assessment of dose calculation accuracy of tigrt treatment planning system for physical wedged fields in radiotherapy. Iran J Med Phys 13(3):146–153
37. Venselaar J, Welleweerd H (2001) Application of a test package in an intercomparison of the photon dose calculation performance of treatment planning systems used in a clinical setting. Radiother Oncol 60(2):203–213
38. Anjum M, Qadir A, Afzal M (2008) Dosimetric evaluation of a treatment planning system using pencil beam convolution algorithm for enhanced dynamic wedges with symmetric and asymmetric fields. Iran J Radiat Res 5(4):169–174
39. Howell RM, Scarboro SB, Kry S, Yaldo DZ (2010) Accuracy of out-of-field dose calculations by a commercial treatment planning system. Phys Med Biol 55(23):6999–7008
40. Huang JY, Followill DS, Wang XA, Kry SF (2013) Accuracy and sources of error of out-of field dose calculations by a commercial treatment planning system for intensity-modulated radiation therapy treatments. J Appl Clin Med Phys 14(2):186–197
41. Mohammadi K, Hassani M, Ghorbani M, Farhood B, Knaup C (2017) Evaluation of the accuracy of various dose calculation algorithms of a commercial treatment planning system in the presence of hip prosthesis and comparison with Monte Carlo. J Cancer Res Ther 13(3):501–509
42. Mahmoudi G, Farhood B, Shokrani P, Amouheidari A, Atarod M (2018) Evaluation of the photon dose calculation accuracy in radiation therapy of malignant pleural mesothelioma. J Cancer Res Ther 14(5):1029–1035
43. Bahreyni Toossi MT, Soleymanifard S, Farhood B, Mohebbi S, Davenport D (2018) Assessment of accuracy of out-of-field dose calculations by TiGRT treatment planning system in radiotherapy. J Cancer Res Ther 14(3):634–639
44. Khan FM, Gibbons JP (2014) Khan's the physics of radiation therapy. Lippincott Williams & Wilkins, Philadelphia
45. Chetty IJ, Curran B, Cygler JE, DeMarco JJ, Ezzell G, Faddegon BA (2007) Report of the AAPM Task Group No. 105: Issues associated with clinical implementation of Monte Carlo-based

photon and electron external beam treatment planning. Med Phys 34(12):4818–4853
46. Swiss Society for Radiobiology and Medical Physics (SGSMP/SSRPM/SSRFM) Quality control of treatment planning systems for teletherapy (1997) Quality control of treatment planning systems for teletherapy. SGSMP Report 7
47. Kilby W, Sage J, Rabett V (2002) Tolerance levels for quality assurance of electron density values generated from CT in radiotherapy treatment planning. Phys Med Biol 47(9):1485–1492